momentum thickness Reynolds number was 4.1×10^3, but did not report any value of L_{22}. Using these anisotropic values of the rms velocity and length scale in Eq. (11) results in the measured 10 dB spread between the low-wave-number longitudinal and transverse spectra. However, in an isotropic model $u_1 = u_2$ and $L_{11} = 2L_{22}$, resulting in only a 3-dB spread. Therefore, the best possible fit for an isotropic model is a $(10-3)/2 = 3.5$ dB underprediction of the longitudinal spectrum and overprediction of the transverse spectrum. This is very close to what is obtained by the CFD-based prediction.

Although the predicted low-wave-number spectrum using the isotropic model has errors of 3–4 dB in a boundary layer, the effect of anisotropy on turbulence ingestion noise calculations is likely to be less significant. This is because unsteady lift is produced by the fluctuating velocity component normal to the blade, which, because of the blade stagger angle, rake, and skew, is generally a combination of u_1, u_2, and u_3 (Ref. 4). Therefore, an isotropic model based on an average of the three velocity components is likely to provide a reasonable approximation of the blade-normal velocity spectrum for rotor turbulence ingestion noise predictions.

V. Conclusions

A model that can be used to predict the turbulence velocity spectrum and correlation function given the k–ε output of a CFD solution has been presented. The model is most accurate in the inertial subrange because of the assumption of isotropy, as demonstrated for a turbulent boundary layer. Because the model is based on the turbulence energy spectrum, it is reasonably independent of the class of flow. For use in predicting turbulence ingestion noise in turbomachinery, the model should provide a reasonable approximation for the entire wave-number range regardless of whether the turbulence is caused by a hull boundary layer, a wake from an upstream obstruction, or a jet from an upstream impeller.

References

[1]Sevik, M., "Sound Radiation from a Subsonic Rotor Subjected to Turbulence," *Fluid Mechanics, Acoustics, and Design of Turbomachinery, Part II*, NASA SP-304, 1974, pp. 493–512.

[2]Thompson, D. E., "Propeller Time Dependent Forces Due to Nonuniform Flow," Ph.D. Dissertation, Dept. of Aerospace Engineering, Pennsylvania State Univ., University Park, PA, May 1976.

[3]Wojno, J. P., Mueller, T. J., and Blake, W. K., "Turbulence Ingestion Noise, Part 2: Rotor Aeroacoustic Response to Grid-Generated Turbulence," *AIAA Journal*, Vol. 40, No. 1, 2002, pp. 26–32.

[4]Gavin, J. R., "Unsteady Forces and Sound Caused by Boundary Layer Turbulence Entering a Turbomachinery Rotor," Ph.D. Dissertation, Graduate Program in Acoustics, Pennsylvania State Univ., University Park, PA, Aug. 2002.

[5]Sears, W. R., "Some Aspects of Non-Stationary Airfoil Theory and Its Practical Application," *Journal of the Aeronautical Sciences*, Vol. 8, 1941, pp. 104–108.

[6]Tennekes, H., and Lumley, J. L., *A First Course in Turbulence*, MIT Press, Cambridge, MA, 1972, Chap. 8.

[7]Hinze, J. O., *Turbulence*, McGraw–Hill, New York, 1975, Chap. 3.

[8]Kolmogorov, A. N., "The Local Structure of Turbulence in Incompressible Viscous Fluid for Very Large Reynolds Numbers," *Doklady Academii Nauk SSR*, Vol. 30, 1941, pp. 301–305; translated by V. Levin and reprinted in *Proceedings of the Royal Society of London, Series A: Mathematical and Physical Sciences*, Vol. 434, 1991, pp. 9–13.

[9]Saddoughi, S. G., and Veeravalli, S. V., "Local Isotropy in Turbulent Boundary Layers at High Reynolds Number," *Journal of Fluid Mechanics*, Vol. 268, 1994, pp. 333–372.

[10]von Kármán, T., "Progress in the Statistical Theory of Turbulence," *Proceedings of the National Academy of Science (USA)*, Vol. 34, 1948, pp. 530–539.

[11]Klebanoff, P. S., "Characteristics of Turbulence in a Boundary Layer with Zero Pressure Gradient," *National Advisory Committee for Aeronautics*, Rept. 1247, U.S. Government Printing Office, Washington, DC, 1956.

W. J. Devenport
Associate Editor

Numerical Simulation of Shock Oscillations over Airfoil Using a Wall Law Approach

E. Goncalvès* and R. Houdeville†
ONERA, 31055 Toulouse CEDEX, France

I. Introduction

SHOCK-INDUCED oscillations (SIO) are a pure aerodynamic problem that can occur over rigid airfoils as a result of the development of instabilities caused by the boundary-layer separation and the shock-wave interaction. This problem is extremely important because it can lead to the buffeting phenomenon through the mechanical response of the wing structure. A detailed description of the physical features of SIO is given by Lee.[1] Computations have been essentielly done over thick airfoils to investigate the SIO problem.[2–4]

Numerically, the local time-step technique, which is efficient to accelerate the convergence towards the steady state, cannot be applied for unsteady computations that imperatively need a global time step. This constraint drastically reduces the method efficiency because of the Courant–Friedrichs–Lewy stability criterion. To overcome this difficulty, the dual time-stepping approach has been proposed by Jameson. It has also been used recently by Furlano et al.[5] and Renaud et al.[6] for SIO computations.

In the present study a wall law approach is used to relax the mesh refinement near the wall and therefore to increase the value of the global time step. Then, the computational efficiency of the explicit method is restored. Providing large CPU cost savings, the wall law approach has also proved to be attractive for the quality of its results in computing separated flows and for the robustness improvment it brings.[7]

Moreover, the eddy viscosity models based on the linear Boussinesq relation are known to be unable to capture the boundary-layer separation and unable to take into consideration the nonequilibrium effects. A consequence of these weakness observed for unsteady computations is the overproduction of eddy viscosity, which limits the development of natural unsteadiness and modifies the flow topology. In this Note, we show that the turbulence model behavior can be remarkably improved by limiting the eddy viscosity with the shear-stress-transport (SST) correction associated with a wall law approach.

II. Numerical Methods

A code solving the uncoupled Reynolds-averaged Navier–Stokes/turbulent systems for multidomain structured meshes is used for the present study. This code is based on a cell-centered finite volume discretization. Fluxes are computed with the Jameson scheme, and time integration is realized through a four-stage Runge–Kutta algorithm. More details about the solver can be found in Ref. 8.

Various two-equation turbulence models are used in the present study: the Menter[9] SST k–ω model and also the high-Reynolds-number version of the Jones–Launder[10] k–ε model, with and without the Menter SST correction.

Presented as Paper 2001-2857 31st Fluid Dynamics Conference, Anaheim, CA, 11–14 June 2001; received 25 July 2001; revision received 10 August 2002; accepted for publication 9 April 2003.

*Assistant Professor, Aerodynamics and Energetics Modelling Department, 2, avenue Belin, B.P. 4025; Eric.Goncalves@hmg.inpg.fr.

†Research Master, Aerodynamics and Energetics Modelling Department, 2, avenue Belin, B.P. 4025; Robert.Houdeville@onecert.fr.

At the wall a no-slip condition is used coupled to a wall law treatment. It consists in imposing the diffusive flux densities, required for the integration process, in adjacent cells to a wall. More details concerning the wall law approach are given in Ref. 7. For unsteady boundary layers the existence of a wall law is assumed valid at each instant. As shown in Cousteix et al.,[11] the velocity phase shift is nearly constant in the logarithmic region and equal to the shift of the wall shear-stress phase. This is true for a Strouhal number up to 10.

III. Flow Conditions

The experimental study has been conducted in the S3MA ONERA wind tunnel[12] with the supercritical RA16SC1 airfoil. The Mach number and the Reynolds number based on the chord are respectively $M_\infty = 0.732$ and $Re_c = 4.2 \times 10^6$. The angle of attack varies from 0 to 4.5 deg. Transition is fixed near the leading edge at $x/c = 7.5\%$ on both sides of the model.

For the computations experimental corrections are used in order to take into account wind-tunnel wall effects. The Mach number is decreased by 0.09, and the angle of attack is decreased by 1 deg at all incidences with respect to experiment. The grid has a C-type topology. It contains 321 nodes, 241 of which are on the airfoil. The y^+ values of the coarse mesh, at the center of the first cell, vary between 1 and 80 for a steady computation at 4-deg angle of attack.

IV. Comparison to Experiments

A. Four-Deg-Incidence, k–ω SST Model

To describe the buffet phenomenon, one period of the lift coefficient is divided into 10 equal parts, as shown in Fig. 1. The skin-friction coefficient $C_{f_0} = \tau_w / 0.5\rho_\infty U_\infty^2$ is plotted in Figs. 2

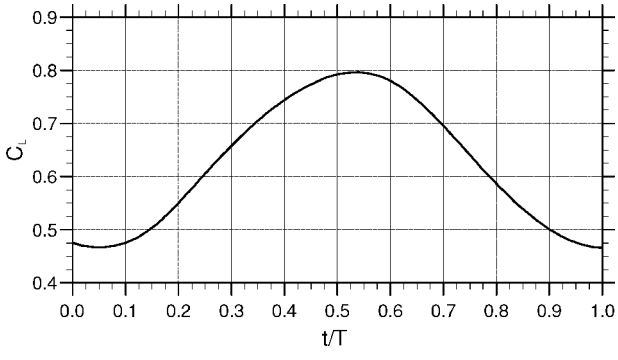

Fig. 1 Lift coefficient over one period of the cycle: 4-deg angle of attack, k–ω with SST correction.

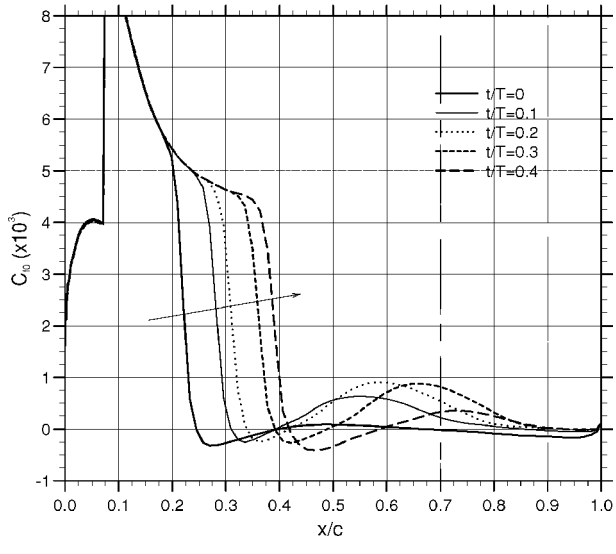

Fig. 2 Skin-friction coefficient during the downward shock displacement: 4-deg angle of attack, k–ω with SST correction.

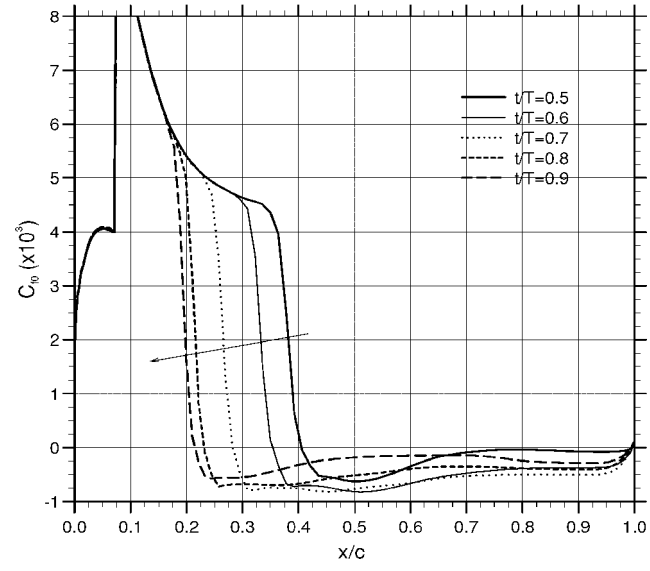

Fig. 3 Skin-friction coefficient during the upward shock displacement: 4-deg angle of attack, k–ω with SST correction.

and 3. At $t/T = 0.5$ when the shock is at the most downstream position, separation occurs at $x/c = 40\%$ without reattachment before the trailing edge, although the backflow intensity is very small after $x/c = 70\%$. As the shock moves upward, the separated region increases and so does the backflow intensity, around $t/T = 0.7$. The magnitude of the negative skin friction does not change a lot during the cycle near the shock. Actually, this change is important on the rear part of the airfoil. When the shock reaches its most upward position, reattachment takes place between $x/c = 40$ and 70%, and the strength of the backflow is strongly reduced. With the downward shock displacement the intensity of the skin friction increases in the reattached region, up to $x/c = 90\%$. A small separation bubble is always present near the foot of the shock.

The development of a mixing layer downstream of the shock can be evidenced by using the Q criterion. During the downward shock displacement, the vortices propagate, with pairing, up to the trailing edge. As the shock moves upward, they are shed in the wake and dissipated very quickly (less than one chord from the trailing edge).

B. Other Results

The rms values of the pressure fluctuations are compared in Fig. 4 with experimental results for three turbulence models and 4-deg angle of attack. The pressure side is represented by the negative values of the abscissa x/c. The maximum value is obtained at $x/c = 40\%$, just after the most downward shock location. The largest discrepancy with experiment is observed downstream the shock location, on the rear part of the airfoil and at the trailing edge.

Figure 4 clearly shows the influence of the SST correction. With the baseline Menter k–ω model no unsteady fluctuations develop at $\alpha = 4$ deg. With the k–ε model shock-induced oscillations exist, but the amplitude of the pressure fluctuations is underestimated. The SST correction increases the oscillation amplitude up to the correct level over all of the suction side. Unfortunately, it also overestimates the pressure fluctuation on the pressure side.

The use of the SST correction and the use of a wall law approach, which removes the wall damping functions in separated regions, are the key points of the present study, both for the numerical efficiency of the time integration and for the quality of the results.

The reduced frequency $2\pi f c/U_\infty$ of the SIO phenomenon and the rms amplitude of the lift coefficient are plotted in Figs. 5 and 6 as a function of the angle of attack. The experiment clearly shows that the reduced frequency increases with incidence. This tendency is reproduced by the computations and particularly well with the k–ω SST model, which gives the reduced frequency within 10% of the experimental results. The k–ε model with SST correction does not seem to render this evolution as well. However, this model correctly

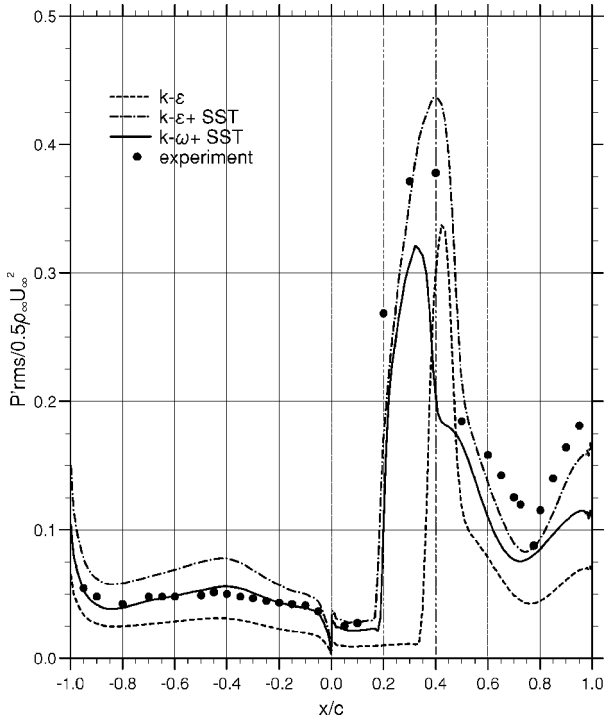

Fig. 4 Rms pressure fluctuations over the airfoil: 4-deg angle of attack, k–ω and k–ε models.

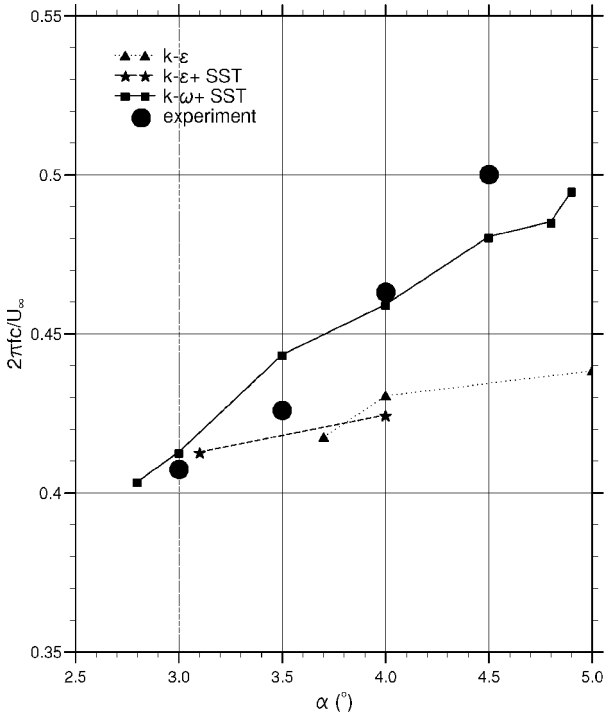

Fig. 5 Reduced frequency parameter vs angle of attack.

predicts the entrance in the SIO domain. Without the SST correction the corresponding angle of attack is shifted by 0.6 deg.

The amplitude of oscillations of the lift coefficient is probably more difficult to compute than the reduced frequency parameter because it directly relies on the correct description of the separated region. The experiment shows that the SIO phenomenon occurs just before the 3-deg angle of attack. The amplitude reaches a maximum value at 4-deg incidence and decreases at larger values. This evolution is remarkably well reproduced by the k–ω SST model, which indicates a return to a steady state at 5-deg incidence. Unfortunately, there are no experimental results at this incidence because

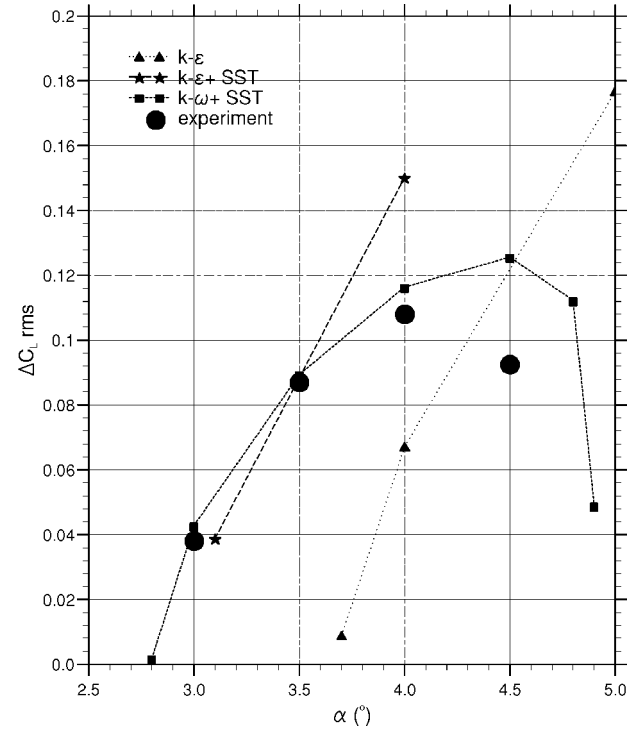

Fig. 6 Amplitude of the lift coefficient fluctuation vs angle of attack.

the emphasis has been put on the buffet appearance. The k–ε model with SST correction also correctly predicts the entrance in the SIO domain but overpredicts the amplitude of oscillations at 4-deg incidence. Without the SST correction the results are shifted by 0.6-deg incidence, as for the reduced frequency parameter.

V. Conclusions

The prediction of shock-induced oscillations has proved to be sensitive to the turbulence modeling and numerical integration methods. The present Note shows the interest of the use of a wall law approach for unsteady computations over a transonic airfoil. First, the numerical efficiency and the CPU cost saving by relaxing the mesh are very significant. Moreover, the treatment associated to the k–ω and k–ε models with the SST limiter is able to predict periodic self-sustained oscillations for the RA16SC1 airfoil correctly. Not only is the frequency of the SIO correctly computed, but also its evolution with the angle of attack as well as the amplitude of the lift coefficient. Comparisons with experimental values of the rms pressure fluctuations clearly indicate the great influence of the SST correction for the quality of results.

References

[1]Lee, B., "Self-Sustained Shock Oscillations on Airfoils at transonic speeds," *Progress in Aerospace Sciences*, Vol. 37, 2001, pp. 147–196.

[2]Raghunathan, S., Gillan, M., Cooper, R., Mitchell, R., and Cole, J., "Shock Oscillations on Biconvex Aerofoils," *Aerospace Science and Technology*, Vol. 3, 1999, pp. 1–9.

[3]Barakos, G., and Drikakis, D., "Numerical Simulation of Transonic Buffet Flows Using Various Turbulence Closures," *International Journal of Heat and Fluid Flow*, Vol. 21, 2000, pp. 620–626.

[4]Wang, D., Wallin, S., Berggren, M., and Eliasson, P., "A Computational Study of Unsteady Turbulent Buffet Aerodynamics," AIAA Paper 2000-2657, June 2000.

[5]Furlano, F., Goncalves, E., Houdeville, R., and Coustols, E., "Unsteady RANS Computations: Simulation of the Buffeting over an Airfoil," IUTAM Symposium on Unsteady Separated Flows, International Union of Theoretical and Applied Mechanics, Toulouse, France, April 2002.

[6]Renaud, T., Corre, C., and Lerat, A., "Efficient Numerical Simulation of Buffet for Airfoils in Transonic Regime," IFASD, Madrid, June 2001.

[7]Goncalves, E., and Houdeville, R., "Reassessment of the Wall Functions Approach for RANS Computations," *Aerospace Science and Technology*, Vol. 5, 2001, pp. 1–14.

[8]Couaillier, V., "Numerical Simulation of Separated Turbulent Flows Based on the Solution of RANS/Low Reynolds Two-Equation Model," AIAA Paper 99-0154, Jan. 1999.

[9]Menter, F., "Two-Equation Eddy-Viscosity Turbulence Models for Engineering Applications," *AIAA Journal*, Vol. 32, No. 8, 1994, pp. 1598–1605.

[10]Jones, W., and Launder, B., "The Prediction of Laminarization with a Two-Equation Model of Turbulence," *International Journal of Heat and Mass Transfer*, Vol. 15, 1972, pp. 301–314.

[11]Cousteix, J., Houdeville, R., and Javelle, J., "Response of a Turbulent Boundary Layer to a Pulsation of the External Flow with and Without Adverse Pressure Gradient," IUTAM Symposium, International Union of Theoretical and Applied Mechanics, Toulouse, France, May 1981.

[12]Benoit, B., and Legrain, I., "Buffeting Prediction for Transport Aircraft Applications Based on Unsteady Pressure Measurements," AIAA Paper 87-2356, Aug. 1987.

R. M. C. So
Associate Editor

Onset of Condensation in Vortical Flow over Sharp-Edged Delta Wing

Satoru Yamamoto*
Tohoku University, Sendai 980-8579, Japan

Introduction

THE actual atmosphere of the Earth includes a finite amount of water vapor, which plays an important role in weather conditions and in the Earth's various environments. Water vapor also plays an interesting role in the flight of airplanes. Water vapor may occasionally condense around the airplane. The phase change may be generally dominated by heterogeneous nucleation of water vapor, because small particulates such as soot or aerosols may behave as a nucleus of condensation.

The condensation around an airplane is the so-called vapor trail. Vapor trails are occasionally observed in the takeoff, landing, and transonic cruising of airplanes. A vapor trail appears as a white cloud over the wing or extending from the wing tip. Campbell et al.[1] summarized a number of photographs of natural condensation.

Because time and space scales in a wind tunnel are fundamentally smaller than those in flight, actual condensation in flight may not be recreated by a flow around a small-scaled wing in the wind tunnel. In atmospheric wind-tunnel conditions, the supersaturation ratio S of water vapor may quickly go beyond the saturation ratio $S = 1$ due to homogeneous nucleation through the inlet of the wind tunnel; it reaches $S \gg 1$ rapidly around the wing without condensation. After this process, a huge amount of water droplets is nucleated in a highly supersaturated condition. This process is dominated by nonequilibrium condensation. As a result, condensation increases temperature and pressure due to the release of the latent heat of water vapor. In atmospheric flight conditions, on the other hand, the chord length of the wing is much longer than that of wind-tunnel models. Furthermore, small particulates, in the atmosphere, such as dust, soot, ions, and aerosols, may play the role of the nucleus for heterogeneous processes. Therefore, actual condensation in flight may be dominated by almost equilibrium condensation.

Received 31 May 2001; presented as Paper 2001-2651 at the AIAA 15th Computational Fluid Dynamics Conference, Anaheim, CA, 11–14 June 2001; revision received 23 April 2003; accepted for publication 12 May 2003.

*Associate Professor, Department of Aeronautics and Space Engineering. Member AIAA.

Recently, Schnerr and Dohrmann[2] studied two-dimensional transonic flows of moist air around an airfoil in atmospheric wind-tunnel conditions experimentally and numerically. Transonic viscous flows of moist air around a NACA0012 airfoil at 2-deg angle of attack in atmospheric wind-tunnel conditions were studied by Iriya et al.[3] Three-dimensional transonic turbulent flows around the ONERA M6 wing were calculated by Yamamoto et al.[4] assuming atmospheric wind tunnel conditions. In this study, the computational code is applied to the calculation of condensation in a streamwise vortex produced over a single delta wing in atmospheric wind-tunnel and flight conditions.

Low-speed flows over a delta wing or a double delta wing at high angle of attack have been widely studied by Hsu et al.,[5] Fujii and Schiff,[6] and Gordnier and Visbal.[7] It is known that a strong streamwise vortex is produced from the apex of the delta wing. All delta-wing studies that we know of have assumed ideal gas without water vapor (zero humidity). However, condensate streamwise vortices are occasionally observed around the delta wing in actual flight.[1] Although condensation is known as quite an important phenomenon affecting wing performance, the physics of condensation in the streamwise vortex over the delta wing is still unknown. Therefore, a study to understand the mechanism underlying the phenomenon would be quite valuable even if it is done at a preliminary level. We provide a preliminary numerical result for the condensation in a streamwise vortex around a delta wing in this Note to further the study of condensate flows in atmospheric flight conditions. As a numerical example, three-dimensional subsonic laminar flows over the 76-deg, sharp-edged single delta wing without thickness at 20.5-deg inclination are calculated under varying inlet or freestream Mach numbers and atmospheric flow conditions, and the onset and the rate of condensation in each flow condition are compared.

Fundamental Equations

The fundamental equations for three-dimensional compressible laminar flows of moist air consist of conservation laws of the total density, the momentums, the total energy, the density of water vapor, the density of liquid water, and the number density of water droplets. This set of equations has been well evaluated in previous studies.[3,4] Flow is supposed to be homogeneous in this study from the assumption that water droplets occurring due to condensation are sufficiently small. Then, velocity slips among air, water vapor, and liquid water are neglected. The equations of state and the speed of sound in this study are those introduced by Ishizaka et al.,[8] assuming that the mass fraction of liquid water, β is sufficiently small ($\beta < 0.1$). These equations are given as follows:

$$p = \rho RT(1-\beta) = \frac{(1-\beta)R}{C_{pm} - (1-\beta)R}\left(e - \frac{1}{2}\rho u_i u_i - \rho h_{0m}\right) \tag{1}$$

$$c = \left[\frac{C_{pm}}{C_{pm} - (1-\beta)R}\frac{p}{\rho}\right]^{\frac{1}{2}} \tag{2}$$

where

$$R = (\rho_a R_u/\rho_g M_a + \rho_v R_u/\rho_g M_v)$$

ρ_a and ρ_g are the densities of dry air and mixed gas; M_a and M_v are the molecular weights of dry air and water vapor, respectively; R_u is the universal gas constant; C_{pm} is defined by the linear combination of the specific heat at constant pressure between gas phase and liquid phase using β; and h_{0m} is the heat of formation.

Condensation Model

In wind-tunnel experiments, onset of condensation may be dominated by homogeneous nucleation,[2] whereas natural condensation observed in the flight of airplanes is governed by heterogeneous nucleation and almost equilibrium condensation. Homogeneous nucleation in this study is based on the classical condensation theory